

Article

Study on Controlled Low-Strength Materials Using Ultra-Rapid-Hardening Cement and Stone Sludge for Backfill and Subbase Application in Road Excavation and Restoration Work

Jongwon Lee and Cheolmin Baek *

Department of Highway and Transportation Research, Korea Institute of Civil Engineering and Building Technology, 283 Goyangdae-ro, Ilsanseo-gu, Goyang-si 10223, Republic of Korea; asca28@kict.re.kr

* Correspondence: cmbaek@kict.re.kr; Tel.: +82-31-910-0613

Abstract: A significant amount of stone sludge is generated as a by-product during the production of crushed stone aggregate, and most of it is disposed of in landfill as waste. In order to recycle this stone sludge, this study evaluated a controlled low-strength material (CLSM) using ultra-rapid-hardening cement and stone sludge for application as backfill and subbase material for road excavation and restoration work. In addition, considering the limited construction time of excavation and restoration work in urban areas, backfill and subbase materials must simultaneously satisfy conditions of fluidity, workability, quick curing time, and certain levels of strength. Therefore, in this study, CLSM was manufactured according to various mixing ratios and flow, slump, and compressive strength tests with age were evaluated. Additionally, the change trend in the microstructure of the CLSM with age was analyzed. Through indoor experiments, the optimal mixing ratios for backfill and subbase CLSM were determined, and field applicability and performance of field samples were evaluated through small-scale field construction. It was concluded that CLSM, which contains a large amount of stone sludge, can be sufficiently applied as a backfill and subbase material for excavation and restoration work if appropriate admixtures are adjusted according to the weather conditions at sites.

Keywords: controlled low-strength materials; road excavation and restoration; ultra-rapid-hardening cement; stone sludge; ettringite formation; field applicability evaluation



Citation: Lee, J.; Baek, C. Study on Controlled Low-Strength Materials Using Ultra-Rapid-Hardening Cement and Stone Sludge for Backfill and Subbase Application in Road Excavation and Restoration Work. *Buildings* **2024**, *14*, 46. <https://doi.org/10.3390/buildings14010046>

Academic Editor: Abdelhafid Khelidj

Received: 10 November 2023

Revised: 9 December 2023

Accepted: 18 December 2023

Published: 22 December 2023



Copyright: © 2023 by the authors. Licensee MDPI, Basel, Switzerland. This article is an open access article distributed under the terms and conditions of the Creative Commons Attribution (CC BY) license (<https://creativecommons.org/licenses/by/4.0/>).

1. Introduction

A large portion of recent road pavement construction in South Korea has been carried out to repair damaged pavement in urban areas. In particular, small-scale excavation and restoration work on urban roads is constantly increasing as the deterioration of underground utilities progresses. Excavation and restoration work in city centers is mainly performed at night due to traffic control restrictions, and same-day excavation and restoration are enforced in principle. Therefore, insufficient compaction occurs due to the insufficient time for sufficient compaction of the backfill layer and subbase layer during the restoration process. This eventually leads to sagging of the restored section and damage to the pavement layer. To solve these problems, backfill materials that have the properties of high flowability, self-compaction, short curing time, and minimum strength for re-excavation are required. Furthermore, it is necessary to investigate mix designs with ultra-rapid-hardening cement or quick-setting agents and mix designs with maximum aggregates to reduce the amount of cement used. However, existing research attempting to resolve these issues is currently insufficient [1].

In the early days of the construction industry, most concrete was produced using river aggregate. However, as river aggregate became scarce, crushed aggregate from quarries began to be used. Currently, crushed aggregate accounts for the largest proportion of

aggregates used in concrete. Quarries produce crushed coarse aggregate and crushed fine aggregate through dry and wet processes. The stone sludge generated through these processes was found to account for approximately 5% of raw stone [2,3]. Based on Korea's crushed aggregate production, the annual stone sludge production is estimated to be more than 15 million tons. Stone sludge can be recycled, but due to transportation and disposal costs, most of it is illegally landfilled or dumped within construction sites [4–6].

In Europe, it was reported that stone sludge generates approximately 5 million tons annually and this amount accounts for about 40% of granite and marble production [7,8]. The environmental pollution caused by large amounts of stone sludge waste has been indicated. Landfills, in particular, have been linked to major contamination of farmland, biota, surface water, and groundwater in countries with less restrictive environmental regulations [9].

To address these problems, many studies have been conducted. In the early 2000s, basic research was conducted on the flowability and strength as a function of water content, admixture ratio, and other parameters, using stone sludge as an admixture [10]. In 2010, various studies were conducted to expand its use by proposing a concrete production and mix design replacing stone sludge with cement and aggregate particulates smaller than 0.08 mm [11–13]. Furthermore, various studies on cement [14,15], mortar [16], concrete [17], gypsum mortar [18], artificial aggregate [19], and asphalt mixtures [20] utilizing stone sludge have shown that the chemical composition of stone sludge directly affects the mechanical properties of final products. Recent studies have succeeded in producing concrete by replacing 10–15% of cement and fine aggregate with stone sludge. They also suggest that stone sludge could be a sustainable waste management option as it enables recycling of natural resources and is a low-carbon material [21–23].

Meanwhile, many road cave-ins, such as sinkholes, which have recently become an issue, are caused by water leaks due to aging and poor construction and management of underground pipes such as sewage and water pipes. Accordingly, in order to solve problems such as difficulty in securing compaction of backfill for underground structures, various studies are being conducted to develop and put into practice controlled low-strength materials (CLSMs), which allow self-filling and self-compaction. CLSMs are made by adding cement or cementitious materials to mud prepared by mixing soil from construction sites and water [24].

Ling et al. examined 115 reports related to CLSM for backfill and found that the materials used to produce CLSM varied across countries. They reported that the use of different materials has a significant impact on CLSM research and field applications [25]. In particular, as CLSM-related research has become more active, more types of industrial waste for CLSM have been researched. Zhang et al. applied fly ash and coal gangue as filler materials and reported that when the ratio was 14:5:1 for gangue, fly ash, and cement, the fluidity of the filler was good and compressive strength was sufficiently developed [26]. Chen et al. evaluated CLSM using coal industry by-products (coal gangue, fly ash, bottom ash, gasification slag, desulfurized gypsum) and cement and showed that it met the criteria of the American Concrete Institute Committee 229 [27]. In particular, in Japan, there are many reports on the characteristics of CLSM using by-products such as low sludge aggregate and glass cullet [28–30]. Horiguchi et al. developed a CLSM by using stone sludge, sludge ash, and sewage. After verifying the mechanical performance of the fabricated CLSM and using it as an actual backfill material for construction, they concluded that sewage, sludge ash, and stone sludge can be used as materials for new CLSMs [31].

In South Korea, as part of technological development toward practical applications of fluidized backfill material for sewer pipes using site-excavated soil generated during construction, a study presented a basic formulation range of CLSM that can respond to site soil by considering engineering properties such as flowability, material separation resistance, early strength, and re-excavation strength [32]. Lee et al. analyzed the physical properties of CLSM by type of sandy clayey excavated soil and mixing factors. The results showed that the mixing conditions needed to meet flowability and early compressive

strength conditions varied even within the same soil classification. This is mainly due to the particle size distribution and fine particle content within the same classification. They reported that the maximum W/B required to meet the flowability and early strength of CLSM utilizing sandy clayey excavated soil was 300% [33]. Kim et al. evaluated the characteristics of CLSMs and derived the optimal mix design for fluidized backfill material for sewer pipes using site-excavated soil generated during construction. Then, they built a batch plant for on-site production to evaluate the re-excavatability and quality sustainability of CLSMs after on-site construction [34].

As a result of reviewing the existing literature, it was found that most CLSM studies were aimed at applications of backfill and did not include stone sludge or used only a small amount. However, in urban road excavation and restoration work, the time for sufficient compaction of not only the backfill layer but also the subbase layer constructed on top of it is limited, causing the problem of sagging after construction. Therefore, the development of backfill and subbase materials that do not require compaction and cure quickly is required. To this end, this study developed and evaluated CLSMs as backfill and subbase materials suitable for urban road excavation and restoration work. In addition, a high percentage of stone sludge was applied to protect natural resources and expand the recycling of industrial by-products. Performance evaluation and microstructure analysis were performed on CLSM for backfill using stone sludge and ultra-fast-hardening cement and on CLSM for subbase by adding coarse aggregate according to various mixing ratios. The field applicability of CLSMs with the derived optimal mixing ratio was evaluated through a small-scale field construction.

2. Materials and Methods

2.1. Stone Sludge

Stone sludge collected from Ewha Aggregate, an aggregate manufacturing plant in Gyeonggi-do South Korea, was used for this study. As a result of evaluating the basic properties, 100% of the stone sludge was found to pass through a 5 mm sieve and 47.54% passed through a 0.075 mm sieve. The maximum dry density was 1.694 g/cm³ and the water content of the stone sludge showed an average of 37.09%, as shown in Table 1.

Table 1. Water content of the stone sludge samples.

Division	Sample-1	Sample-2	Sample-3
Wet soil (g)	525	802	731
Dry soil (g)	383	582	536
Water (g)	142	220	195
Water content (%)	37.08	37.80	36.38
Average water content (%)		37.09	

2.2. Cement

Ordinary Portland cement from domestic company “Hanil” was used in this study and Table 2 shows the physical properties and chemical composition ratio of this cement.

Table 2. Characteristics of ordinary Portland cement.

Density (g/cm ³)	Fineness (cm ² /g)	Chemical Composition (%)						
		SiO ₂	Al ₂ O ₃	Fe ₂ O ₃	CaO	MgO	SO ₃	Ig.Loss
3.14	3492	21.1	4.64	3.14	62.8	2.81	2.13	2.18

2.3. Ultra-Rapid-Hardening Cement

For the development of backfill material utilizing stone sludge, ultra-rapid-hardening cement manufactured by domestic Company J was used in this study. The physicochemical properties are presented in Table 3. The ultra-rapid-hardening cement used in this study

belongs to the category of specialty cement, which develops a strength of 30–40% of its ultimate strength (4 MPa) in less than 4 h of aging.

Table 3. Characteristics of the ultra-rapid-hardening cement.

Density (g/cm ³)	Fineness (cm ² /g)	Chemical Composition (%)						
		SiO ₂	Al ₂ O ₃	Fe ₂ O ₃	CaO	MgO	SO ₃	Ig.Loss
3.00	5070	3.02	23.19	0.45	46.15	0.43	24.14	1.24

2.4. Coarse Aggregate

A crushed granite aggregate was used for coarse aggregate. The particle size was between 5 mm and 25 mm, and Table 4 shows the physical properties of the coarse aggregate.

Table 4. Coarse aggregate properties.

Density (g/cm ³)	Absorption (%)	Unit Weight (kg/m ³)	Fineness Modulus	Sound (%)
2.72	0.74	1664	7.03	3.09

2.5. Admixtures

In this study, superplasticizer and retarder were used to improve the workability of the CLSMs and to ensure adherence to working time constraints. Tables 5 and 6 present the physicochemical properties of the superplasticizer and retarder.

Table 5. Properties of superplasticizer.

Ingredient	pH	Density (g/cm ³)	Evaporation Residual Rate (%)
Polycarboxylate	5.5	0.5	84

Table 6. Properties of the retarder.

Ingredient	pH	Density (g/cm ³)	Purity (%)
Tartaric acid	7.0~8.5	0.31	95

2.6. CLSM for Backfill Material

2.6.1. Mix Proportion

Based on the results of the properties of the backfill material in the preliminary study and the economic feasibility, a mix design of the backfill material using ultra-rapid-hardening cement and stone sludge was created as shown in Table 7 [24]. The OPC-1 mix using normal Portland cement was included for comparison with the mix using ultra-rapid-hardening cement. For URHC-1, 2, and 3, the quantity of admixture was adjusted to achieve excellent workability and adhere to working time constraints through flow measurement. Furthermore, the compressive strength of the backfill material after 2 h, 4 h, and 1 day was measured to observe the initial strength development and the compressive strength at 7, 14, and 28 days was measured to examine the strength-increasing trend. The test also included the case of the URHC-4 mix, where the amount of stone sludge was increased to reduce the quantity of cement at 300% W/B.

Table 7. Mix proportion.

Test ID	W/B (%)	Binder Type	Weight Unit (kg/m ³)			Weight Composition (%/B)	
			Water	Binder	Stone Sludge	P.C.	R.T.
OPC-1	300	Cement	594	250	580	-	-
URHC-1		Ultra-rapid-hardening cement	594	250	580	0.20	0.20
URHC-2			594	250	580	0.30	0.20
URHC-3			503	236	752	0.30	0.20
URHC-4			503	236	752	0.30	0.20

2.6.2. Flow Test

The flowability of CLSMs in this study was evaluated according to ASTM D 6103 (Standard Test Method for Flow Consistency of Controlled Low Strength Material) [35]. Figure 1 shows the fabrication and measurement of a CLSM flow test specimen.



Figure 1. Flow test.

2.6.3. Compressive Strength Test

ASTM D 4832 (Standard Test Method for Preparation and Testing of Controlled Low Strength Material (CLSM Test Cylinders)) [36] was applied to measure the compressive strength of the CLSMs. Cylindrical specimens, measuring 100 mm in height and 50 mm in diameter, were prepared using a 2:1 cylinder-type mold. The testing temperature was 20 ± 5 °C. The CLSM specimens and testing setup are shown in Figure 2.



Figure 2. Specimens and test setup for compressive strength test.

2.7. CLSM for Subbase Material

2.7.1. Mix Proportion

The mix proportion for the subbase layer utilizing stone sludge and coarse aggregate was derived from the CLSM mix for backfill material. The mixing quantity of coarse aggregate was 40 Vol.% of the total volume of stone sludge and coarse aggregate. The mixing equipment is shown in Figure 3, and the mix proportion is shown in Table 8.



Figure 3. Mixing of CLSM.

Table 8. Mix proportions.

Test ID	W/B (%)	Binder Type	Weight Unit (kg/m ³)				Weight Composition (%/B)	
			Water	Binder	Stone Sludge	Aggregate	P.C.	R.T.
URHC-5	300	Ultra-rapid-hardening cement	489	206	478	478	0.30	0.20
URHC-6			394	185	588	588		

2.7.2. Slump Test

To examine the workability of CLSM for the subbase layer using stone sludge, coarse aggregate and ultra-rapid-hardening cement, a slump test was conducted according to KS F 2402 (Test Method for Concrete Slump) [37] as with the slump test for concrete. The test setup is shown in Figure 4.



Figure 4. Slump test.

2.7.3. Compressive Strength Test

The compressive strength was measured using cylindrical specimens of $\phi 100 \times 200$ mm, as shown in Figure 5, according to KS F 2405 (Test Method for Compressive Strength of Concrete) [38]. Specimens were tested at 20 ± 5 °C by measuring 2-h, 4-h, and 1-day compressive strength values to observe initial strength development. Furthermore, 7-, 14-, and 28-day compressive strength values were measured to examine strength-increasing trends.

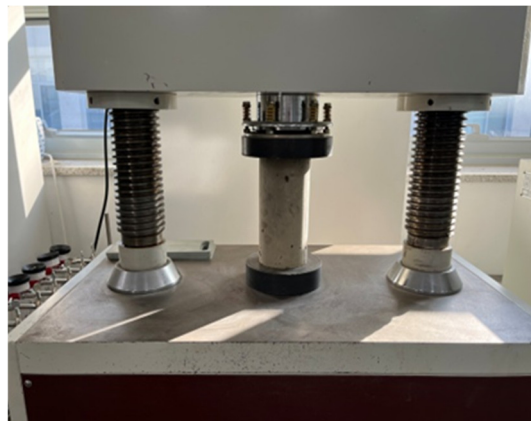


Figure 5. Compressive strength test.

2.8. Microstructure Analysis

2.8.1. SEM and EDS

The microstructure of CLSMs containing stone sludge was analyzed using scanning electron microscopy (SEM). The equipment used was a Merlin Compact (Carl Zeiss, Oberkochen, Germany) equipped with an in-lens detector and various signal processing functions. Additionally, the elemental composition of the surface of CLSM particles was analyzed using energy-dispersive X-ray spectroscopy (EDS).

2.8.2. XRD

Materials generated from the hydration reaction of CLSMs were analyzed using X-ray diffraction (XRD). The equipment used was Bruker's 1 Dimensional LYNXEYE detector and a D8 Advance diffractometer (Billerica, MA, USA). Samples were scanned in the 2θ range of 5° – 95° with a step size of 0.01° and a time of 1 s per step. Qualitative analysis was performed by obtaining XRD patterns for CLSM specimens and standard specimens under identical conditions.

3. Results

3.1. CLSM for Backfill Material

3.1.1. Flow Test Result

The flow test results of the CLSM for backfill material utilizing ultra-rapid-hardening cement and stone sludge are as shown in Figure 6. The OPC-1 with normal Portland cement did not show any decrease in flow with the mixing time. However, in the case of the URHC-1 mix using ultra-rapid-hardening cement with no admixture, the flow rate tended to decrease after 5 min of mixing time. In contrast, URHC-2, 3, and 4 showed a very sharp decrease in flow rate when the mixing time exceeded 10 min. URHC-2 and URHC-3 showed a difference of about 80 mm, depending on the quantity of superplasticizer used. Moreover, both mix proportions showed similar trends of decreasing flow with mixing time. It was determined that with an increasing quantity of superplasticizer, the flow increased due to the separation of particles resulting from the increased free water, among the free water, adsorbent bed water, and recharge water that affected the flow in the cement matrix [39]. The flow of URHC-4 was measured lower than the other mix proportions. This is thought to be due to the reduced free water and increased adsorbent bed water

resulting from the relatively increased stone sludge in the URHC-2 and URHC-3 mixes, which can have a negative impact on flowability [40]. Using a retarder of 0.2% by weight of ultra-rapid-hardening cement resulted in a mixing time of about 10 min. Thus, it is necessary to increase the retarder to adhere to time constraints according to the work situation, and the superplasticizer needs to be increased to improve the work performance.

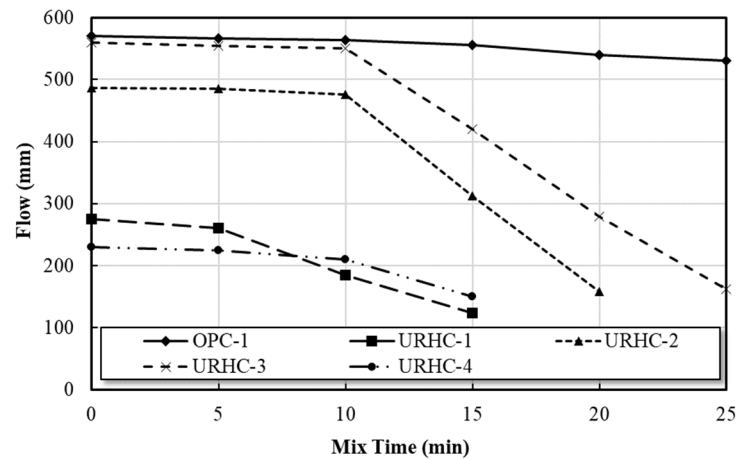


Figure 6. Flow test result of CLSM for backfill material.

3.1.2. Compressive Strength Test Results

Figure 7 shows the compressive strengths by age of CLSM for backfill material utilizing ultra-rapid-hardening cement and stone sludge. OPC-1, which used ordinary Portland cement as a binder, did not cure until 4 h, making it impossible to demold the specimen, and strength measurement was possible from 1 day of age. The compressive strength was low at 0.84 MPa even at 28 days of age due to the relatively high W/B. When ultra-rapid-hardening cement was used, all mix proportions showed an initial strength higher than 0.14 MPa, which is sufficient for open traffic during the backfilling of buried pipes [41]. The compressive strength values of URHC-1, 2, and 3 were rapidly increased from 2 h to 7 days after the initial strength measurement. At 28 days of age, they exhibited a more moderate increase in strength with values of 2.01, 1.98, and 1.96 MPa, respectively. The compressive strength tended to decrease as the amount of superplasticizer increased. Although the fluidity increased due to the increase in free water caused by the superplasticizer, the free water consumed in the CLSM hydration reaction for backfill material was left as pores. This led to a relatively large volume of pores, reducing its strength. Adding a retarder can inhibit the hydration reaction of ultra-rapid-hardening cement for a while. However, when the hydration reaction was initiated after some time, the final compressive strength did not significantly change due to the exothermic action of hydration by chemical reaction. Regarding compressive strength, the increase in superplasticizer decreased the compressive strength, but the difference was insignificant, and the effect of retarder was insignificant [42]. URHC-4 with an increased amount of stone sludge at the same W/B showed excellent strength properties in every mix proportion. This is because although the amount of binder was relatively reduced, the increase in stone sludge lowered the flowability, and the strength increased because the hydration reaction was initially active. Thus, considering the flowability and strength properties of backfill material mixed with ultra-rapid-hardening cement and stone sludge, the most adequate mix proportions were thought to be URHC-3 and URHC-4 with a W/B of 300%, 0.3% superplasticizer (wt./B), and 0.2% retarder (wt./B) using ultra-rapid-hardening cement as the binder.

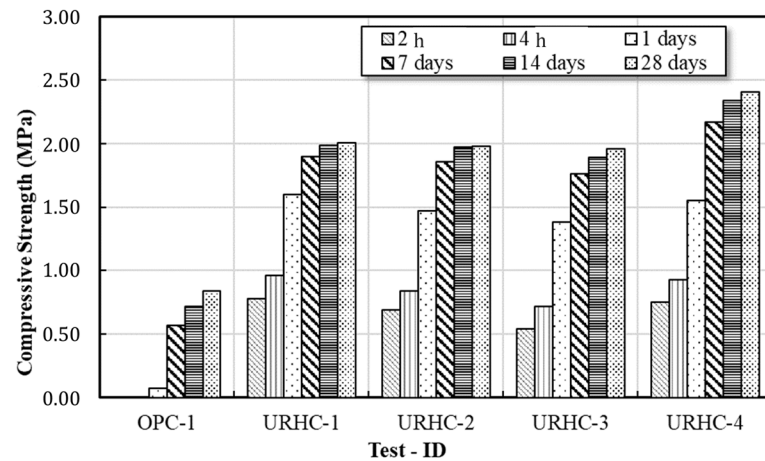


Figure 7. Compressive strength test result of CLSM for backfill material.

3.2. CLSM for Subbase Material

3.2.1. Slump

The target slump of the CLSM for subbase layers utilizing ultra-rapid-hardening cement, stone sludge, and coarse aggregate was set at 170 ± 10 mm considering the flowability and workability. The slump test results showed that 20 min of mixing time was required for URHC-5 to achieve the targeted flowability. The slump could not be measured before achieving the target slump due to increased flowability, as shown in Figure 8, and material separations occurred partially. URHC-6, which reduced the quantity of binder and increased the quantity of stone sludge, took around 5 min to mix. A sharp deterioration in flowability occurred about 10 min after achieving the target slump, as shown in Figure 9. Thus, pouring should be performed immediately after adequate mixing.



Figure 8. Slump test of URHC-5.



Figure 9. Slump test of URHC-6.

3.2.2. Compressive Strength Test

To analyze the compressive strength of CLSM for subbase layers utilizing ultra-rapid-hardening cement, stone sludge, and coarse aggregate, the specimens were prepared with the target slump. Figure 10 shows the results of the compressive strength test by age. Both URHC-5 and URHC-6 mixes, which included 40% of coarse aggregate, showed compressive strength values of more than 0.9 MPa at 2 h and more than 1.0 MPa at 4 h. This ensured a compressive strength of 0.7 MPa for the following process (asphalt layer paving). For the URHC-6 mix, the quantity of stone sludge was increased to reduce the unit amount of binder. Thus, it showed a greater compressive strength because the amount of water initially added was relatively reduced and the hydration reaction was active at an early stage, shortening the mixing time to achieve the target slump. Therefore, URHC-6 is thought to be adequate as a CLSM mix for subbase layers to complete pipeline construction in the city center targeted in this study within the specified time, considering both workability and compressive strength.

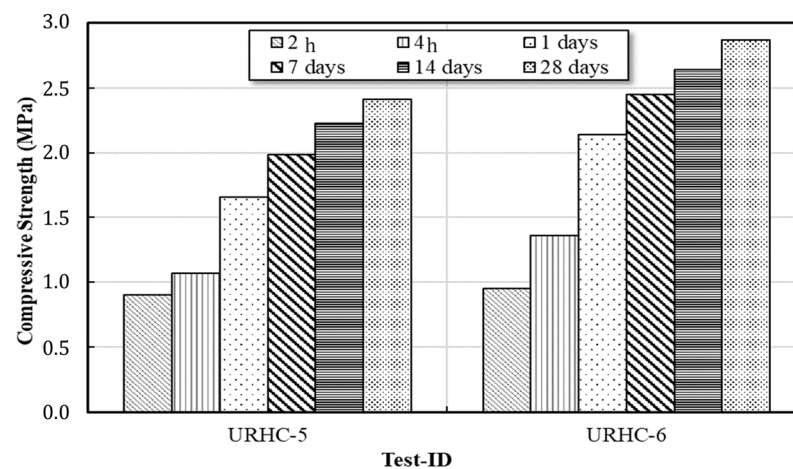


Figure 10. Compressive strength test result of CLSM for subbase material.

3.3. Microstructure Analysis Results

3.3.1. SEM and EDS Analysis Results

CLSM specimens were taken at 2 h, 1 day, 7 days, 14 days, and 28 days of age and analyzed by SEM and EDS. Figures 11 and 12 show the results of microstructure analysis. The CLSM that used ultra-rapid-hardening cement as a binder initially showed a large quantity of ettringite and dense microstructures. Furthermore, as the age increased, the density of internal microstructures increased because the hydration reaction with the cement became more active. In the early stage, a large quantity of ettringite was observed. The mechanism of strength development of ultra-rapid-hardening cement is that in the presence of SO_3 , Ca^{2+} ions eluting immediately after contact with water and Al^{3+} ions eluting from calcium aluminate react to produce calcium aluminate hydrate ($\text{CaO} \cdot \text{Al}_2\text{O}_3 \cdot n\text{H}_2\text{O}$). Then, this reacts with gypsum in the cement to produce ettringite ($3\text{CaO} \cdot \text{Al}_2\text{O}_3 \cdot 3\text{CaSO}_4 \cdot 32\text{H}_2\text{O}$), which hardens rapidly, resulting in early strength development [43]. Consequently, a large quantity of ionic components such as Al, O, Ca, and S were detected in the 2 h EDS mapping as shown in Figure 11. Furthermore, the high fineness compared to ordinary cement is highly reactive when mixed with water, causing an active hydration reaction. As a result, the reaction that produces the hydrate of ettringite occurs more rapidly. This suggests that the flow value was measured lower and the compressive strength was higher compared to ordinary cement. The mix proportion with ultra-rapid-hardening cement showed a large amount of ettringite and C–S–H and C–A–H gels at 7 days of age as shown in Figure 12. In addition, on the $\text{Ca}(\text{OH})_2$ surface, thin sheet-shaped C–S–H gel appeared widely distributed. This indicates that as $\text{Ca}(\text{OH})_2$ was consumed, secondary ettringite was formed and C–S–H and C–A–H gels were generated at 7 days of age. At 28 days of age, as

C–S–H gel and C–A–H gel were generated in large quantities around the ettringite nucleus, it was confirmed that the internal structure was stabilizing by filling the micropores of CLSM using ultra-fast-hardening cement and stone sludge.

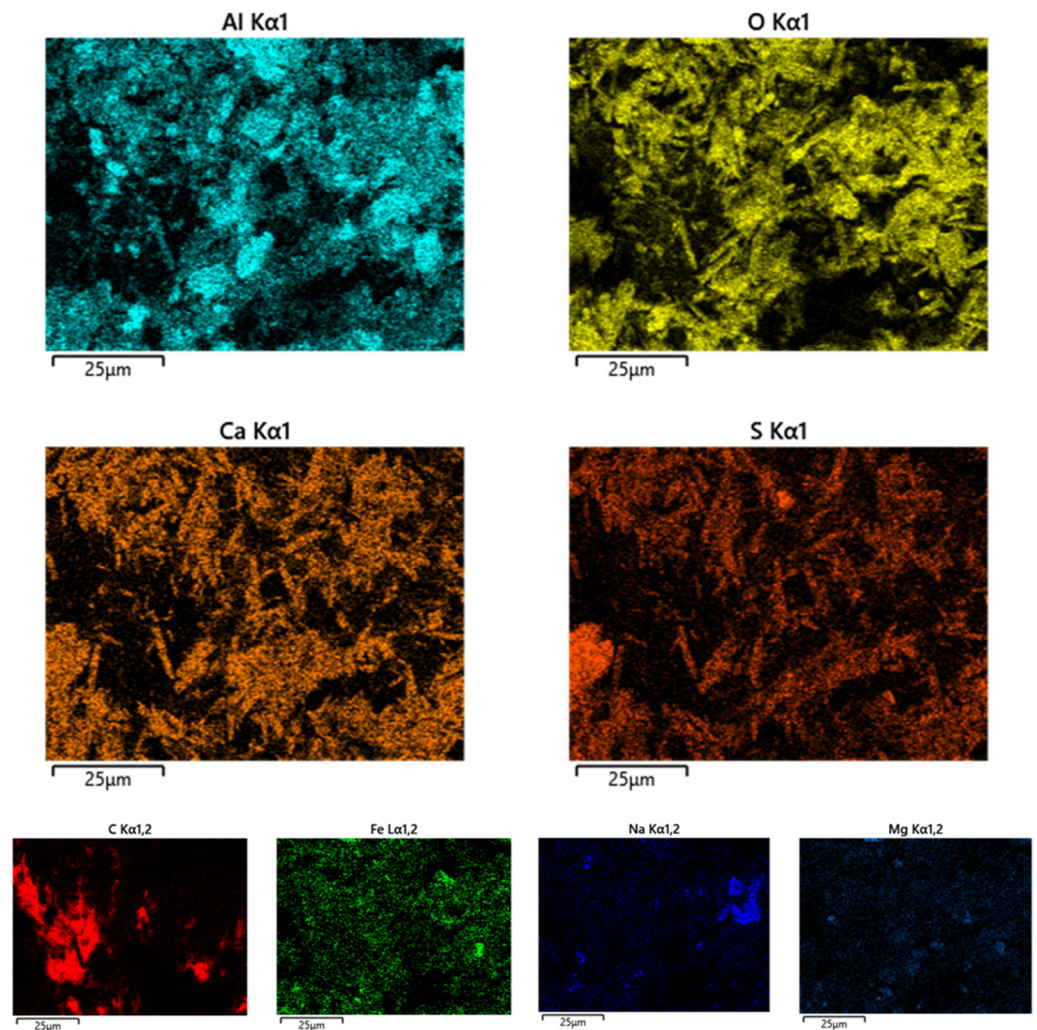
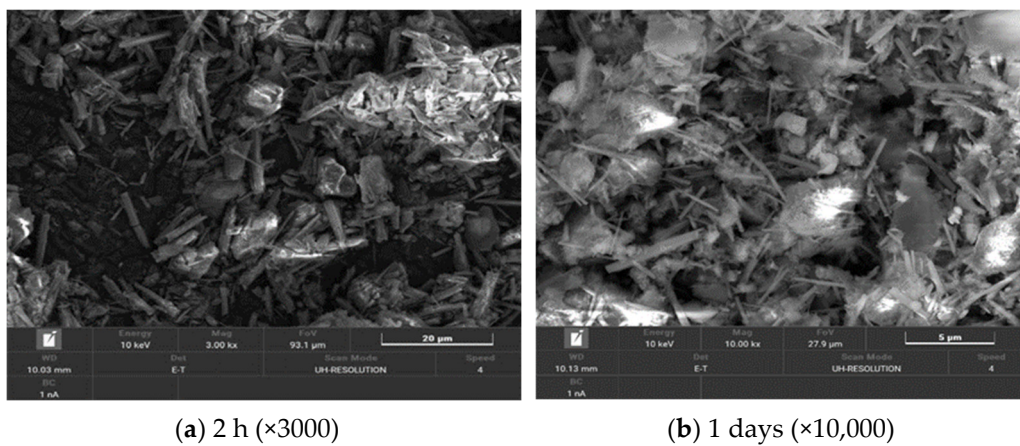


Figure 11. EDS mapping result of CLSM using URHC.



(a) 2 h ($\times 3000$)

(b) 1 days ($\times 10,000$)

Figure 12. Cont.

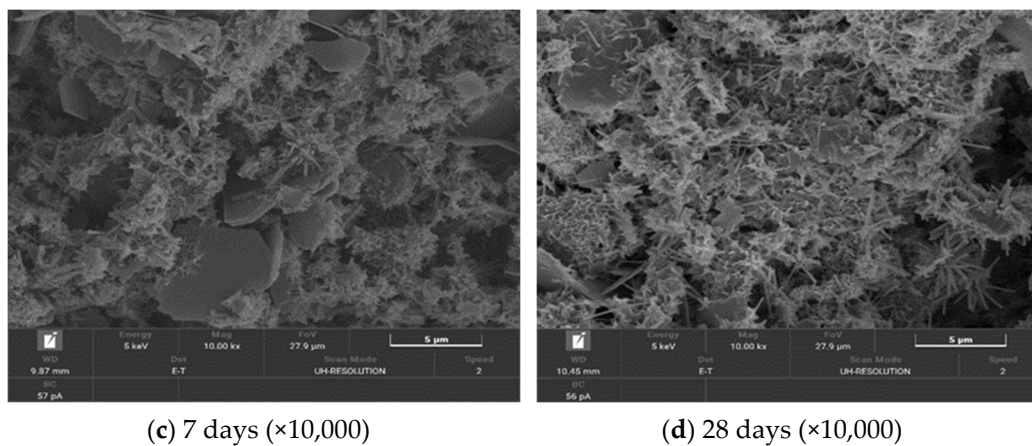


Figure 12. SEM image of CLSM using URHC.

3.3.2. XRD Analysis Results

Figure 13 shows the XRD analysis results of a sample collected at 28 days of CLSM using stone sludge and ultra-rapid-hardening cement. The peak of SiO_2 became more evident in the mix using stone sludge. The CLSM with ordinary Portland cement showed very low peaks except for ettringite. This is thought to be due to the relatively high W/B, which inhibited the smooth hydration reaction. The CLSM with ultra-rapid-hardening cement confirmed ettringite, C-S-H, and C-A-H gel hydrate, as shown by SEM. In particular, the ettringite peak clearly appeared in the mix using ultra-rapid-hardening cement. This is determined to be due to the hydration reaction characteristics of ultra-rapid-hardening cement, as described in Section 3.3.1. Furthermore, Al_2O_3 in ultra-rapid-hardening cement and SiO_2 , which is the main component of stone sludge, cause pozzolanic reactions with CH in the cement matrix, and this accelerates the hydration reaction compared to ordinary cement [44,45]. As a result, mixing proportions with ultra-rapid-hardening cement may produce more C-S-H and C-A-H. The C-S-H and C-A-H are generated through pozzolanic reaction and they are attached to the surface of stone sludge, and the density within the CLSM matrix increases, thereby reducing harmful voids [46].

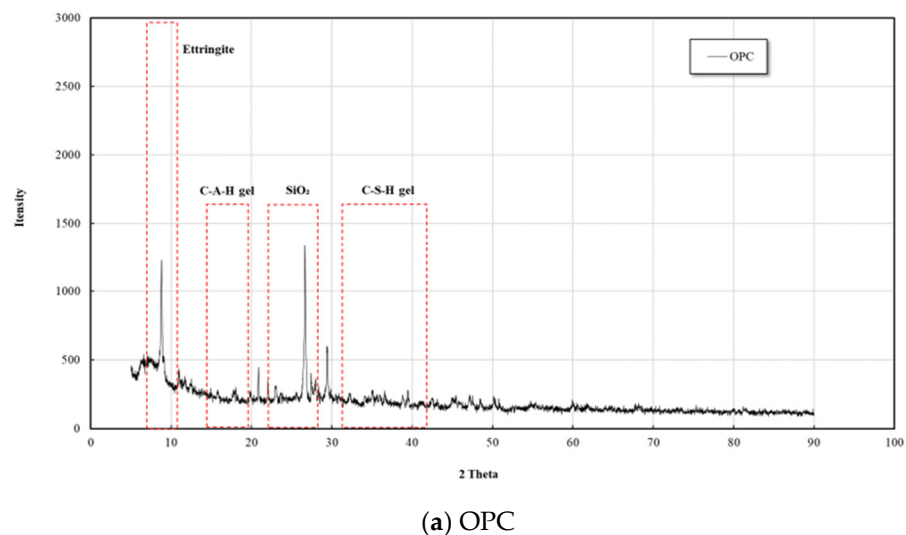
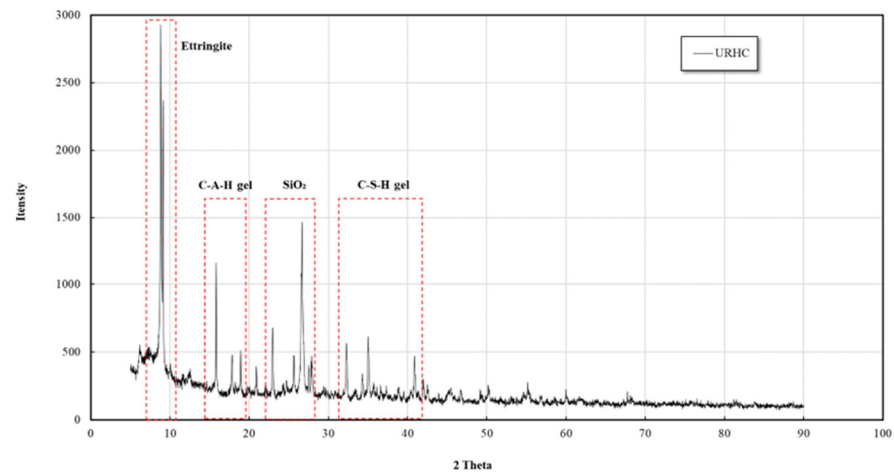


Figure 13. Cont.



(b) URHC

Figure 13. 28-day XRD results for different binders.

4. Evaluation of Field Applicability for CLSMs

4.1. Site Construction Overview

A field construction evaluation was carried out by applying the optimal mix proportions of URHC-3 and URHC-6 derived from the indoor experimental evaluation. This process is shown in Figure 14. The mixer used for the on-site production and pouring of CLSMs was a piece of dedicated CLSM equipment developed as part of this study.



(a) Excavation



(b) Concrete pipe installation



(c) Pilot mixer for CLSM



(d) CLSM mixing

Figure 14. Cont.



(e) Backfill CLSM construction



(f) Subbase CLSM construction

Figure 14. Photographs of the field construction of the CLSMs.

As shown in Figure 15, before pouring the CLSM for each mix, a slump test and a flow test were conducted to characterize the CLSMs, and specimens were fabricated in the field. In addition, to evaluate the constructability of the upper layer after construction of CLSM material, the change in hardness of the CLSM layer was measured through a soil penetrometer test and a Kelly ball test.



(a) Flow test for backfill CLSM



(b) Specimen fabrication for backfill CLSM



(c) Slump test for subbase CLSM



(d) Specimen fabrication for subbase CLSM



(e) Soil penetrometer test



Figure 15. *Cont.*



(f) Kelly ball test

Figure 15. Photographs of the field test of the CLSMs.

4.2. Field Evaluation Result

4.2.1. Evaluation of Mechanical Properties

The flow test result of CLSM for backfill satisfied the ASTM D 4832 standard [36] of 200 mm or more, as shown in Table 9. Furthermore, the slump test result of CLSM for subbase layers showed a target slump of 170 ± 10 mm, as shown in Table 10. In addition, both CLSMs were found to have excellent workability during field construction. As shown in Table 9, the compressive strength of CLSM for backfill was greater than 0.6 MPa after 2 h. The compressive strength of CLSM for subbase layers was larger than 1.0 MPa after 2 h as shown in Table 10. The field test results showed lower flowability and increased compressive strength compared to the indoor test. This difference occurred because of the change in the water content due to the use of a large amount of stone sludge and the performance difference between the mixer used in the indoor test and the mixer used in the field test [47,48].

Table 9. Flow and compressive strength test result of CLSM for backfill.

NO.	Flow (mm)	Compressive Strength (MPa, 2 h)
1	360	0.66
2	370	0.67
3	360	0.63
Average	363.3	0.65

Table 10. Slump and compressive strength test result of CLSM for subbase layers.

NO.	Slump (mm)	Compressive Strength (MPa, 2 h)
1	165	1.14
2	161	1.01
3	160	1.12
Average	162	1.09

4.2.2. Review of Subsequent Process Initiation of CLSMs

To examine the possibility of subsequent processing of backfill material, an evaluation was conducted with a soil hardness meter in accordance with ASTM D 6024, Standard Test Method for Ball Drop on Controlled Low Strength Material (CLSM) to Determine Suitability for Load Application [49], and Tokyo Metropolitan Construction Bureau Quality Standards for Fluidized Treated Soil [50]. The construction area was divided into four zones, and each zone was evaluated every 10 min. The results are summarized in Tables 11 and 12.

Table 11. Soil penetrometer test result of backfill material.

NO.	Soil Penetrometer (mm)					
	10 min	20 min	30 min	40 min	50 min	60 min
1	1.2	2.1	3.1	3.7	4.2	5.2
2	1.3	2.0	3.3	3.9	4.3	5.3
3	1.3	2.8	3.4	3.7	4.1	4.9
4	1.4	2.2	3.5	4.1	4.5	5.5
Average	1.30	2.28	3.33	3.85	4.28	5.23

NO.	Kelly Ball (mm)					
	10 min	20 min	30 min	40 min	50 min	60 min
1	130.8	123.1	100.5	95.4	82.2	70.5
2	131.5	120.9	107.2	98.0	87.9	75.3
3	132.6	128.1	96.6	93.7	88.8	74.7
4	130.9	120.2	103.3	90.1	84.5	74.0
Average	131.45	123.08	101.90	94.30	85.85	73.63

Table 12. Soil penetrometer test result of subbase material.

NO.	Soil Penetrometer (mm)					
	10 min	20 min	30 min	40 min	50 min	60 min
1	1.3	2.7	3.5	4.2	4.9	6.2
2	1.5	2.7	3.6	4.8	5.6	6.7
3	1.6	2.4	3.8	4.5	5.3	6.3
4	1.6	2.6	3.4	4.3	5.5	5.9
Average	1.5	2.6	3.58	4.45	5.33	6.28

NO.	Kelly Ball (mm)					
	10 min	20 min	30 min	40 min	50 min	60 min
1	125.8	108.5	95.2	82.4	73.9	69.5
2	126.3	115.4	99.5	85.1	74.6	70.2
3	132.6	121.3	104.2	86.4	78.1	73.5
4	128.5	118.5	103.8	90.8	79.8	72.5
Average	128.3	115.93	100.68	86.18	76.6	71.43

As a result of the hardness characteristics of the backfill CLSM over time, by using a soil hardness meter, penetration was measured at 4.28 mm at 50 min after pouring, meeting the standard value (more than 3 mm). The penetration of subbase CLSM was measured to be 4.45 mm after 40 min, about 10 min earlier than the backfill CLSM, meeting the standard (more than 3 mm). As a result of the Kelly ball test, the backfill CLSM and subbase CLSM values were found to be 73.63 mm and 71.43 mm, respectively, about 1 h after pouring, so both CLSM met the standard (75 mm or less).

5. Conclusions

In this study, the engineering properties and microstructures of CLSMs for backfill and subbase layers using ultra-rapid-hardening cement, stone sludge, and coarse aggregate were analyzed. Additionally, small-scale field construction and testing were performed to evaluate the field applicability of CLSMs. The following conclusions were drawn through this study:

- (1) For the backfill CLSM using stone sludge and ultra-rapid-hardening cement, the addition of superplasticizer and retarder is inevitable considering the working environment of urban centers. Considering the flowability and early compressive strength, the most adequate mix proportion for backfill CLSM is URHC-3 with a W/B of 300%, 0.3% (wt./B) superplasticizer, and 0.2% (wt./B) retarder, using an ultra-rapid-hardening cement as the binder;

- (2) For the subbase CLSM using ultra-rapid-hardening cement, stone sludge, and coarse aggregate, it should be poured immediately after appropriate mixing due to the decrease in flowability with mixing time. Therefore, URHC-6 is judged to be suitable for subbase CLSM mixes used to complete pipe construction in urban areas within a given time, considering both workability and compressive strength;
- (3) The microstructure analysis results showed that the primary hydration reaction of CLSM for backfill and subbase layers provided primary initial strength by generating ettringite. Subsequently, the internal structure of the CLSM was stabilized and the strength was enhanced as C–S–H and C–A–H gels were generated around SiO₂, the main component of the stone sludge, and the primary ettringite nucleus;
- (4) As a result of small-scale field construction of CLSMs, it was found that they were sufficiently applicable to the field in terms of constructability and performance. However, compared to the indoor test, fluidity was lowered and compressive strength was increased. This is because the moisture content of stone sludge and the performance of the mixer used in the field are different from those in the laboratory. Therefore, the quantity of admixture used and the water content of the stone sludge need to be verified through a water content experiment, considering weather conditions before mixing.

Author Contributions: Conceptualization, C.B.; methodology, J.L. and C.B.; validation, J.L. and C.B.; formal analysis, J.L. and C.B.; investigation, J.L. and C.B.; resources, J.L. and C.B.; data curation, J.L. and C.B.; writing—original draft preparation, J.L.; writing—review and editing, C.B.; visualization, J.L.; supervision, C.B.; project administration, C.B.; funding acquisition, C.B. All authors have read and agreed to the published version of the manuscript.

Funding: This work was supported by the Korea Agency for Infrastructure Technology Advancement (KAIA) grant funded by the Ministry of Land, Infrastructure and Transport (Grant No. 22POQWB152342-01).

Data Availability Statement: The data presented in this study are available in the article.

Conflicts of Interest: The authors declare no conflict of interest.

References

1. Han, S.H.; Yang, S.L.; Lee, J.W.; Back, C.M. Evaluation of fugitive dust emission generated by construction process of pavement excavation-restoration through the field test. *Int. J. Highw. Eng.* **2020**, *22*, 61–68. [[CrossRef](#)]
2. Jeong, J.S.; Lee, J.C.; Yang, K.Y.; So, K.H. Utilization of stone sludge produced by stone block manufacturing process as concrete admixtures. *J. Korea Inst. Build. Constr.* **2008**, *8*, 83–89. [[CrossRef](#)]
3. Han, C.G.; Shin, B.C.; Kim, G.C.; Lee, S.T. Strength and absorption properties of cement mortar produced with various content of sludge powder at mines. *J. Korea Concr. Inst.* **2001**, *13*, 561–567.
4. Ko, D.; Choi, H. Basic performance evaluation of dry mortar recycled basalt powder sludge. *J. Korea Inst. Build. Constr.* **2013**, *13*, 131–138. [[CrossRef](#)]
5. Jeong, J.Y.; Choi, S.M.; Kawg, E.G.; Choi, S.J.; Lee, S.Y.; Kim, J.M. The Strength Properties of Concrete Used Stone Powder Sludge as Siliceous Material. In Proceedings of the Korean Institute of Building Construction Conference, Seoul, Republic of Korea, 1 May 2005; pp. 85–88.
6. Galetakis, M.; Soutana, A. A review on the utilization of quarry and ornamental stone industry fine by-products in the construction sector. *Constr. Build. Mater.* **2016**, *102*, 769–781. [[CrossRef](#)]
7. Graziani, A.; Giovannelli, G.I.L. *Lapidei Struttura del Settore e Tendenze Innovative*; Centro Studi Fillea: Rome, Italy, 2015. Available online: http://www.filleacgil.it/nazionale/accordi/all_1817.pdf (accessed on 10 June 2020). (In Italian)
8. Zichella, L.; Bellopede, R.; Spriano, S.; Marini, P. Preliminary investigations on stone cutting sludge processing for a future recovery. *J. Clean. Prod.* **2018**, *178*, 866–876. [[CrossRef](#)]
9. Nasseridine, K.; Mimi, Z.; Bevan, B.; Elian, B. Environmental management of the stone cutting industry. *J. Environ. Manag.* **2009**, *90*, 466–470. [[CrossRef](#)]
10. Lim, S.Y.; Song, J.H.; Jaung, J.D. A study on properties of general strength-high folw concrete using sludge of crushed stone. *J. Archit. Inst. Korea* **2006**, *26*, 409–412.
11. Song, J.W.; Choi, J.J. The influence of fine particles under 0.08 mm contained in aggregate on the characteristics of concrete. *J. Korea Concr. Inst.* **2013**, *25*, 347–354. [[CrossRef](#)]
12. Seo, J.Y.; Choi, S.J.; Kang, S.T. Physical effect of adding stone dust sludge on the properties of cement mortar. *J. Korean Recycl. Constr. Resour. Inst.* **2015**, *3*, 152–158.

13. Hong, K.N.; Lee, J.H.; Han, S.H.; Park, J.K. Mechanical properties of concrete using crushed stone sludge as substitutes. *J. Inst. Constr. Technol.* **2012**, *31*, 79–84.
14. Mashaly, A.O.; Shalaby, B.N.; Rashwan, M.A. Performance of mortar and concrete incorporating granite sludge as cement replacement. *Constr. Build. Mater.* **2018**, *169*, 800–818. [[CrossRef](#)]
15. Mashaly, A.O.; El-Kaliouby, B.A.; Shalaby, B.N.; El-Gohary, A.M.; Rashwan, M.A. Effects of marble sludge incorporation on the properties of cement composites and concrete paving blocks. *J. Clean. Prod.* **2016**, *112*, 731–741. [[CrossRef](#)]
16. Lozano-Lunar, A.; Dubchenko, I.; Bashynskiy, S.; Rodero, A.; Fernández, J.M.; Jiménez, J.R. Performance of self-compacting mortars with granite sludge as aggregate. *Constr. Build. Mater.* **2020**, *251*, 118998. [[CrossRef](#)]
17. Sardinha, M.; de Brito, J.; Rodrigues, R. Durability properties of structural concrete containing very fine aggregates of marble sludge. *Constr. Build. Mater.* **2016**, *119*, 45–52. [[CrossRef](#)]
18. Nascimento, A.S.S.; Santos, C.P.; Melo, F.M.C.; Oliveira, V.G.A.; Betânio Oliveira, R.M.P.; Macedo, Z.S.; Oliveira, H.A. Production of plaster mortar with incorporation of granite cutting wastes. *J. Clean. Prod.* **2020**, *265*, 121808. [[CrossRef](#)]
19. Chang, F.C.; Lee, M.Y.; Lo, S.L.; Lin, J.D. Artificial aggregate made from waste stone sludge and waste silt. *J. Environ. Manag.* **2010**, *91*, 2289–2294. [[CrossRef](#)] [[PubMed](#)]
20. Choudhary, J.; Kumar, B.; Gupta, A. Feasible utilization of waste limestone sludge as filler in bituminous concrete. *Constr. Build. Mater.* **2020**, *239*, 117781. [[CrossRef](#)]
21. Dobiszewska, M.; Bagcal, O.; Beycioğlu, A.; Goulias, D.; Köksal, F.; Płominski, B.; Ürünveren, H. Utilization of rock dust as cement replacement in cement composites: An alternative approach to sustainable mortar and concrete productions. *J. Build. Eng.* **2023**, *69*, 106180. [[CrossRef](#)]
22. Karalar, M.; Özkılıç, Y.O.; Aksoylu, C.; Sabri, M.M.S.; Beskopylny, A.N.; Stel'makh, S.A.; Shcherban, E.M. Flexural behavior of reinforced concrete beams using waste marble powder towards application of sustainable concrete. *Front. Mater.* **2022**, *9*, 1068791. [[CrossRef](#)]
23. Zeybek, Ö.; Özkılıç, Y.O.; Karalar, M.; Çelik, A.I.; Qaidi, S.; Ahmad, J.; Burduhos-Nergis, D.D.; Burduhos-Nergis, D.P. Influence of replacing cement with waste glass on mechanical properties of concrete. *Materials* **2022**, *15*, 7513. [[CrossRef](#)]
24. Lee, J.W.; Baek, C. Microstructure analysis and mechanical properties of backfill material using stone sludge. *Materials* **2023**, *16*, 1511. [[CrossRef](#)]
25. Ling, T.C.; Kaliyavaradhan, S.K.; Poon, C.S. Global perspective on application of controlled low-strength material (CLSM) for trench backfilling—An overview. *Constr. Build. Mater.* **2018**, *158*, 535–548. [[CrossRef](#)]
26. Zhang, Q.L.; Wu, X.M. Performance of cemented coal gangue backfill. *J. Cent. South Univ.* **2007**, *14*, 216–219. [[CrossRef](#)]
27. Chen, T.; Yuan, N.; Wang, S.; Hao, X.; Zhang, X.; Wang, D.; Yang, X. The effect of bottom ash ball-milling time on properties of controlled low-strength material using multi-component coal-based solid wastes. *Sustainability* **2002**, *14*, 9949. [[CrossRef](#)]
28. Adaska, W.S. Controlled low-strength materials. *Concr. Int.* **1997**, *19*, 41–43.
29. Horiguchi, T.; Okumura, H.; Saeki, N. *Durability of CLSM with Used Foundry Sand, Bottom Ash, and Fly Ash in Cold Regions*; American Concrete Institute: Farmington Hills, MI, USA, 2001.
30. Horiguchi, T.; Saeki, N. Compressive strength and leachate characteristic of new green CLSM with eco-cement and melted slag from municipal solid waste. In *8th Canmet/ACI Fly Ash Conf.*; Malhotra, V.M., Ed.; American Concrete Institute: Farmington Hills, MI, USA, 2004; pp. 539–558.
31. Horiguchi, T.; Fujita, R.; Shimura, K. Applicability of controlled low-strength materials with incinerated sewage sludge ash and crushed-stone powder. *J. Mater. Civ. Eng.* **2011**, *23*, 767–771. [[CrossRef](#)]
32. Lea, D.H.; Nguyen, K.H. An assessment of eco-friendly controlled low-strength material. *Sustain. Dev. Civ. Urban Transp. Eng.* **2016**, *142*, 260–267. [[CrossRef](#)]
33. Lee, J.; Kim, Y.W.; Lee, B.C.; Jung, S.H. Engineering properties of controlled low strength material for sewer pipe by standard soil classification. *J. Rec. Const. Resour.* **2018**, *6*, 182–189.
34. Kim, Y.W.; Lee, B.C.; Jung, S.H. Field applicability assessment of controlled low strength material for sewer pipe using excavated soil. *J. Korean Recycl. Constr. Resour. Inst.* **2019**, *7*, 349–357.
35. ASTM D6103-17; Standard Test Method for Flow Consistency of Controlled Low Strength Material (CLSM). ASTM International: West Conshohocken, PA, USA, 2017. Available online: https://www.astm.org/d6103_d6103m-17.html (accessed on 18 June 2022).
36. ASTM D4832-16e1; Standard Test Method for Preparation and Testing of Controlled Low Strength Material (CLSM) Test Cylinders. ASTM International: West Conshohocken, PA, USA, 2018.
37. KS F 2402; Test Method for Concrete Slump. Korean Standards Association: Seoul, Republic of Korea, 2022.
38. KS F 2405; Test Method for Compressive Strength of Concrete. Korean Standards Association: Seoul, Republic of Korea, 2022.
39. Zhao, M.; Zhang, X.; Zhang, Y. Effect of free water on the flowability of cement paste with chemical or mineral admixtures. *Constr. Build. Mater.* **2016**, *111*, 571–579. [[CrossRef](#)]
40. Luo, F.J.; He, L.; Pan, Z.; Duan, W.H.; Zhao, X.L.; Collins, F. Effect of very fine particles on workability and strength of concrete made with dune sand. *Constr. Build. Mater.* **2013**, *47*, 131–137. [[CrossRef](#)]
41. Japan Civil Engineering Research Institute. Technical Notes of Fluidization Surplus Soil. 2007.
42. Kim, G.M.; Choi, J.; Bang, J.; Jung, J.; Park, S.W.; Yang, B. Effect of artificial interior stone sludge on physicochemical properties of mortars. *J. Build. Eng.* **2023**, *75*, 106949. [[CrossRef](#)]

43. Gwon, S.; Jang, S.Y.; Shin, M. Microstructure evolution and strength development of ultra rapid hardening cement modified with redispersible polymer powder. *Constr. Build. Mater.* **2018**, *192*, 715–730. [[CrossRef](#)]
44. Qing, Y.; Zenan, Z.; Deyu, K.; Rongshen, C. Influence of nano-SiO₂ addition on properties of hardened cement paste as compared with silica fume. *Constr. Build. Mater.* **2007**, *21*, 539–545. [[CrossRef](#)]
45. Meng, T.; Yu, Y.; Qian, X.; Zhan, S.; Qian, K. Effect of nano-TiO₂ on the mechanical properties of cement mortar. *Constr. Build. Mater.* **2012**, *29*, 241–245. [[CrossRef](#)]
46. Atta-ur-Rehman; Qudoos, A.; Kim, H.G.; Ryou, J.-S. Influence of titanium dioxide nanoparticles on the sulfate attack upon ordinary portland cement and slag-blended mortars. *Materials* **2018**, *11*, 356. [[CrossRef](#)]
47. Liao, X.K.; Kim, D.H. Field applicability evaluation of control low strength materials as utilizing various industrial by-products. *J. Rec. Const. Resour.* **2020**, *8*, 387–394.
48. Bae, Y.S.; Sin, S.Y.; Won, J.S.; Lee, D.H. *The Road Subsidence Condition and Safety Improvement Plans in Seoul*; The Seoul Institute Working Paper 2016-PR-09; The Seoul Institute: Seoul, Republic of Korea, 2016.
49. *ASTM D6024*; Standard Test Method for Ball Drop on Controlled Low Strength Material (CLSM) to Determine Suitability for Load Application. ASTM International: West Conshohocken, PA, USA, 2017.
50. Tokyo Metropolitan Construction Bureau. *Quality Standards for Fluidized Treated Soil*; Tokyo Metropolitan Construction Bureau: Tokyo, Japan, 2009.

Disclaimer/Publisher's Note: The statements, opinions and data contained in all publications are solely those of the individual author(s) and contributor(s) and not of MDPI and/or the editor(s). MDPI and/or the editor(s) disclaim responsibility for any injury to people or property resulting from any ideas, methods, instructions or products referred to in the content.